Inverse Elastic Scattering Problem

Shiqi Zhou

Chinese Academy of Science, Academy of Mathematics and System Science

2018.11.13 Zhejiang Lab

Content

Motivation

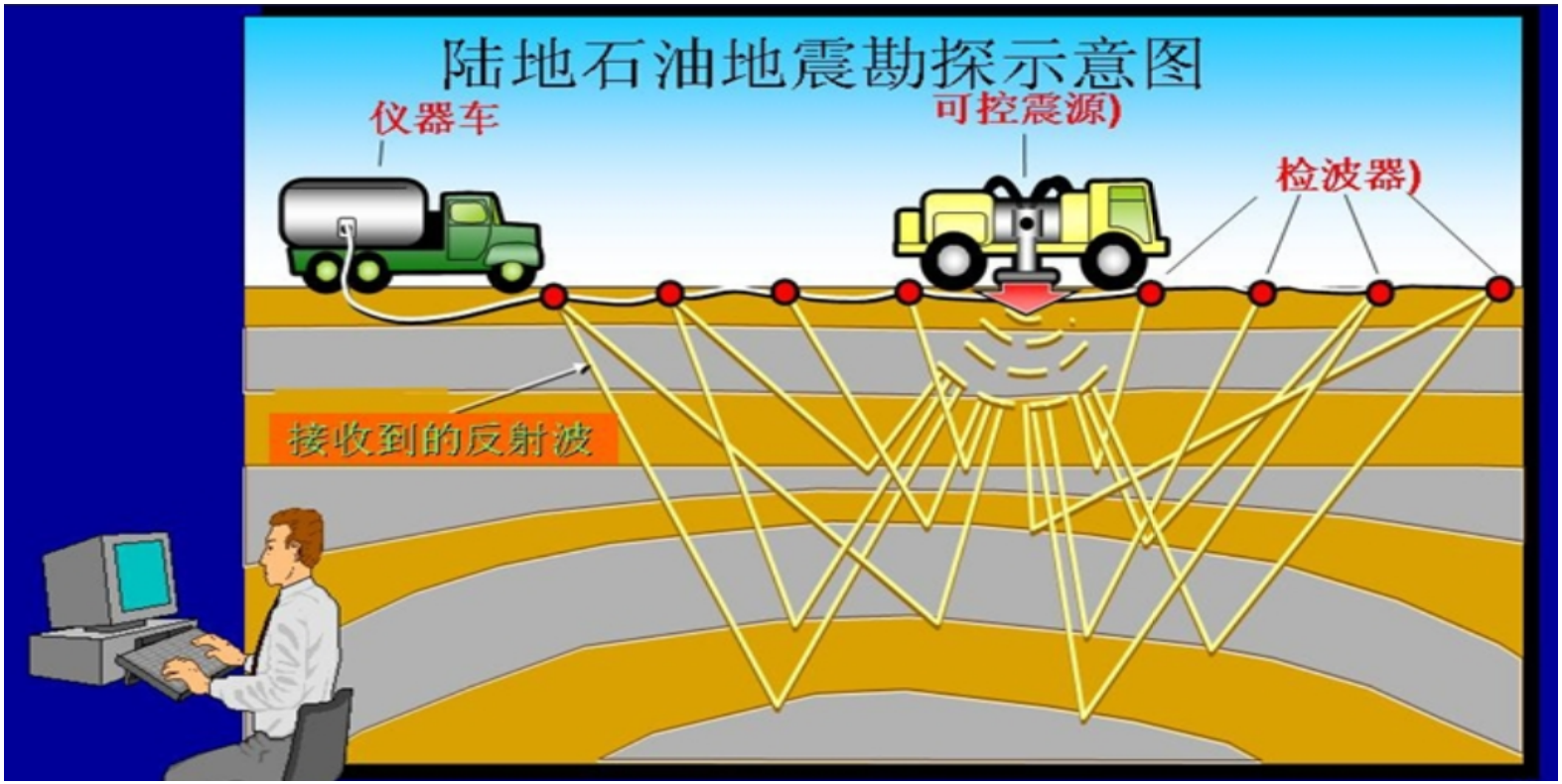

Figure: Find the support of the unknown obstacle from the knowledge of the scattered waves on a given surface.

Direct Scattering Problem in the Half Space

We consider elastic wave propagating in the half space with Neumann condition(Traction Free),

$$\nabla \cdot \sigma(u_q) + \rho\omega^2 u_q = -\delta_{x_s}(x)q \quad \text{in } \mathbb{R}^2_+ \backslash \bar{D}$$
$$u_q = 0 \ \text{ on } \Gamma_D \ \text{ and } \ \sigma(u_q) \cdot e_2 = 0 \ \text{ on } \Gamma_0$$

together with the constitutive relation (Hookes law)

$$\sigma(u) = 2\mu\varepsilon(u) + \lambda \mathrm{div} u \mathbb{I}$$
$$\varepsilon(u) = \frac{1}{2}(\nabla u + (\nabla u)^T)$$

where ω is the circular frequency, $u(x) \in \mathbb{C}^2$ denotes the displacement fields and $\sigma(u)$ is the stress tensor. We also need to define the surface traction $T^n_x(\cdot)$ on the normal direction n,

$$T^n_x u(x) := \sigma \cdot n = 2\mu \frac{\partial u}{\partial n} + \lambda n \mathrm{div} u + \mu n \times \mathrm{curl} u$$

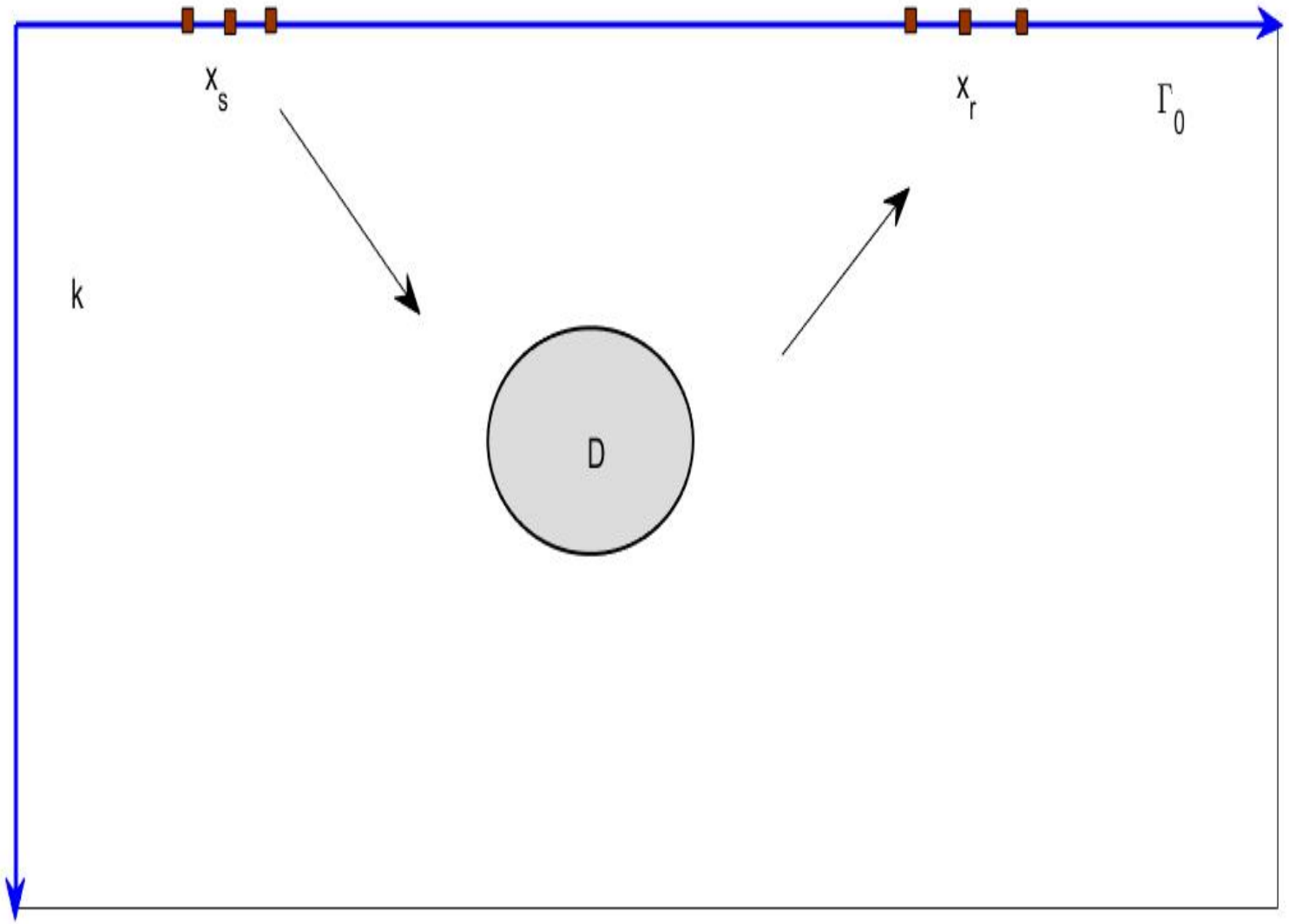
x_s
x_r
Γ_0
k
D

Green Tensor in the Half Space

Green Tensor in the half-space with Neumann boundary :

$$\begin{aligned} \Delta_e \mathbb{N}(x;y) + \omega^2 \mathbb{N}(x,y) &= -\delta_y(x)\mathbb{I} \quad \text{in} \quad \mathbb{R}^2_+, \\ \sigma_x(\mathbb{N}(x,y))e_2 &= 0 \qquad \text{on} \quad x_2 = 0 \end{aligned}$$

Green Tensor in the half-space with Dirichlet Boundary

$$\begin{aligned} \Delta_e \mathbb{D}(x,y) + \omega^2 \mathbb{D}(x,y) &= -\delta_y(x)\mathbb{I} \quad \text{in} \quad \mathbb{R}^2_+, \\ \mathbb{D}(x,y) &= 0 \qquad \text{on} \quad x_2 = 0 \end{aligned}$$

where $\delta_y(x)$ is the Dirac source at $y \in R^2_+$ and $N(x,y)$, $\mathbb{D}(x,y)$ are $\mathbb{C}^{2\times 2}$ matrixes.

Remark: we will assume that for $z \in \mathbb{C}$, $z^{1/2}$ is the analytic branch of $\sqrt{z}$ such that $\mathrm{Im}\,(z^{1/2}) \geq 0$.

Green Tensor in Frequency Domain after Fourier Transformation

$$\hat{\mathbb{N}}(\xi, x_2; y_2) = \hat{\mathbb{G}}(\xi, x_2; y_2) - \hat{\mathbb{G}}(\xi, x_2; -y_2) + \hat{\mathbb{N}}_c(\xi, x_2; y_2)$$

$$\begin{aligned}\hat{\mathbb{N}}_c(\xi, x_2; y_2) = \quad = \quad & \frac{\mathbf{i}}{\omega^2 \delta(\xi)} \Big\{ A(\xi) e^{\mathbf{i}\mu_s (x_2 + y_2)} + B(\xi) e^{\mathbf{i}\mu_p (x_2 + y_2)} \\ & + C(\xi) e^{\mathbf{i}\mu_s x_2 + \mu_p y_2} + D(\xi) e^{\mathbf{i}\mu_p x_2 + \mu_s y_2} \Big\}\end{aligned}$$

where $\mathbb{G}(x, y)$ is the fundamental solution of elastic equation and

$$A(\xi) = \begin{pmatrix} \mu_s \beta^2 & -4\xi^3 \mu_s \mu_p \\ -\xi \beta^2 & 4\xi_4 \mu_p \end{pmatrix} \qquad B(\xi) = \begin{pmatrix} 4\xi^4 \mu_s & \xi \beta^2 \\ 4\xi^3 \mu_s \mu_p & \mu_p \beta^2 \end{pmatrix}$$

$$C(\xi) = \begin{pmatrix} 2\xi^2 \mu_s \beta & -2\xi \mu_s \mu_p \beta \\ -2\xi^3 \beta & 2\xi^2 \mu_p \beta \end{pmatrix} \quad D(\xi) = \begin{pmatrix} 2\xi^2 \mu_s \beta & 2\xi^3 \beta \\ 2\xi \mu_s \mu_p \beta & 2\xi^2 \mu_p \beta \end{pmatrix}$$

and $\mu_\alpha = (k_\alpha^2 - \xi^2)^{1/2}$, $\alpha \in \{s, p\}$, $\beta(\xi) = k_s^2 - 2\xi^2$, $\delta(\xi) = \beta^2 + 4\xi^2 \mu_s \mu_p$.

Dirichlet Green Tensor in Frequency Domain after Fourier Transformation

$$\hat{\mathbb{D}}(\xi, x_2; y_2) = \hat{\mathbb{G}}(\xi, x_2; y_2) - \hat{\mathbb{G}}(\xi, x_2; -y_2) + \hat{M}(\xi, x_2; y_2)$$

$$\begin{aligned} \hat{M}(\xi, x_2; y_2) \quad = \quad & \frac{\mathbf{i}}{\omega^2 \gamma(\xi)} \Big\{ A(\xi) e^{\mathbf{i}\mu_s (x_2 + y_2)} + B(\xi) e^{\mathbf{i}\mu_p (x_2 + y_2)} \\ & - A(\xi) e^{\mathbf{i}\mu_s x_2 + \mu_p y_2} - B(\xi) e^{\mathbf{i}\mu_p x_2 + \mu_s y_2} \Big\} \end{aligned}$$

where

$$A(\xi) = \begin{pmatrix} \xi^2 \mu_s & -\xi \mu_s \mu_p \\ -\xi^3 & \xi^2 \mu_p \end{pmatrix} \qquad B(\xi) = \begin{pmatrix} \xi^2 \mu_s & \xi^3 \\ \xi \mu_s \mu_p & \xi^2 \mu_p \end{pmatrix}$$

and $\gamma(\xi) = \xi^2 + \mu_s \mu_p$.

Lemme 1

Let *Lamé* constant $\lambda, \mu \in \mathbb{R}^+$, then the Rayleigh equation $\delta(\xi) = 0$ has only two roots denoted by $\pm k_R$ in complex plane. Morever, $k_R > k_s > k_p,\ k_R \in \mathbb{R}$ and k_R is called Rayleigh wave number.

Using Cauchy integral theorem, we carry out:

Formula 1

$$\mathbb{N}(x,\, y) = \frac{1}{2\pi}\mathrm{P.V}\int_{\mathbb{R}} \hat{\mathbb{N}}(\xi,\, x_2;\, y_2)e^{\mathbf{i}(x_1-y_1)\xi}\, d\xi - \frac{\mathbf{i}}{2}\frac{\mathbb{N}_\delta(-k_R)}{\delta'(-k_R)}e^{-\mathbf{i}(x_1-y_1)k_R} + \frac{\mathbf{i}}{2}\frac{\mathbb{N}_\delta(k_R)}{\delta'(k_R)}e^{\mathbf{i}(x_1-y_1)k_R}$$

where $\mathbb{N}_\delta(\xi) = \hat{\mathbb{N}}(\xi, x_2; y_2)\delta(\xi)$.

Lemma 2

Let *Lamé* constant $\lambda, \mu \in \mathbb{C}$ and $\mathrm{Im}\,(k_s) \geq 0, \mathrm{Im}\,(k_p) \geq 0$, then equation $\gamma(\xi) = 0$ has no root in complex plane.

Formula 2

Let $\mathbb{T}_D(x, y)$ denote the traction of $\mathbb{D}(x, y)$ in direction e_2 with respect to x such that $\mathbb{T}_D(x, y)e_i = \sigma_x(\mathbb{D}(x, y)e_i)e_2$.

$$\mathbb{T}_D(x, y) = \mathbb{T}(x, y) - \mathbb{T}(x, y') + \frac{1}{2\pi}\int_{\mathbb{R}} \hat{\mathbb{T}}_M(\xi, x_2; y_2)e^{\mathbf{i}(x_1 - y_1)\xi} d\xi$$

and

$$\hat{\mathbb{T}}_M(\xi, x_2; y_2) = \frac{\mu}{\omega^2\gamma(\xi)}\Big\{E(\xi)e^{\mathbf{i}\mu_s(x_2+y_2)} + F(\xi)e^{\mathbf{i}\mu_p(x_2+y_2)} - E(\xi)e^{\mathbf{i}\mu_s x_2+\mu_p y_2} - F(\xi)e^{\mathbf{i}\mu_p x_2+\mu_s y_2}\Big\}$$

where

$$E(\xi) = \begin{pmatrix} -\xi^2\beta & \xi\mu_p\beta \\ 2\xi^3\mu_s & -2\xi^2\mu_s\mu_p \end{pmatrix} \quad F(\xi) = \begin{pmatrix} -2\xi^2\mu_s\mu_p & -2\xi^3\mu_p \\ -\xi\mu_s\beta & -\xi^2\beta \end{pmatrix}$$

Inverse Scarttering Problem

$$\begin{cases} \nabla \cdot \sigma(u_q) + \rho\omega^2 u_q = -\delta_{x_s}(x)q & in \quad \mathbb{R}^2_+ \setminus \bar{D} \\ u_q = 0 & on \quad \Gamma_D \\ \sigma(u_q) \cdot e_2 = 0 & on \quad \Gamma_0 \end{cases}$$

satisfies the generalized radiation condition

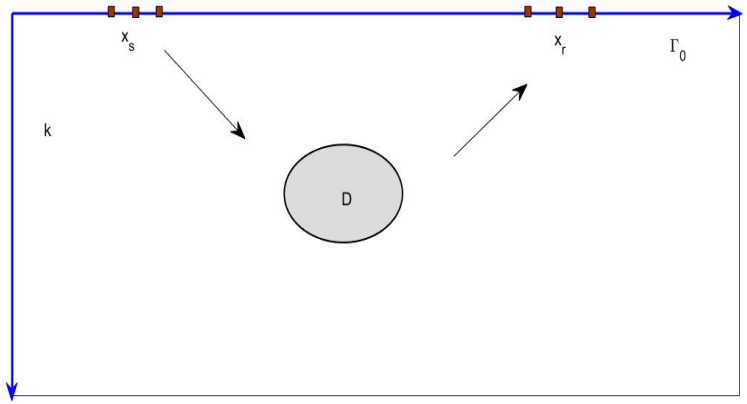

Direct Problem

To determine the scattering wave field $u^s(x, x_s) = u(x, x_s) - u^i(x, x_s)$ from the given incident field $u^i(x, x_s) = \mathbb{N}(x, x_s)$, the differential equation governing the wave motion and the information of obstacle.

Inverse problem

To determine the location, size, sharp of the obstacle by the measured field $u^s(x, x_s)$ on x_r

Algorithms of inverse obstacle problem

Direct Imaging Method

- Linear Sample MethodFactorization methodPoint source method
- MUltiple SIgnal Classification
- Prestack depth migrationReverse Time Migration

Feature

Fast computationDifficult mathematics analysis

Iterative Method

- Differential semblance optimization
- Full waveform inversion
- Recursive linearization algorithm

Feature

Need prior information, Difficult to convergence, Provide quantitative information

Reverse Time Migration

- Do not require any priori information of the physical properties of the obstacle such as penetrable or non-penetrable, and for non-penetrable obstacles, the type of boundary conditions on the boundary of the obstacle.
- The previous analysis of the migration method is usually based on the high frequency assumption so that the geometric optics approximation can be used.

Reverse Time MigrationMathematics Framework

Acoustic, electromagnetic, elastic wave in the Full space

1. Chen J, Chen Z, Huang G. *Reverse time migration for extended obstacles: acoustic waves [J]*. Inverse Problems. 2013, 29(8):645-648
2. Chen J, Chen Z, Huang G. *Reverse time migration for extended obstacles: Electromagnetic waves[J]*. Scientia Sinica, 2015, 29(8):085005.
3. Chen Z, Huang G. *Reverse time migration for extended obstacles: Elastic waves (in Chinese)[J]*. Science China Mathematics, 2015, 45(8):1103-1114.

Planar acoustic waveguide

1. Chen Z M, Huang G H. *Reverse time migration for reconstructing extended obstacles in planar acoustic waveguides[J]*. Science China Mathematics, 2015, 58(9):1811-1834.

Acoustic in the Half space

1. Chen Z, Huang G. *Reverse time migration for reconstructing extended obstacles in the half space[J].* Inverse Problems, 2015, 31(5):055007 (19pp).

Phaseless Algorithm

1. Chen Z, Huang G. *Phaseless Imaging by Reverse Time Migration: Acoustic Waves[J].* Numerical Mathematics Theory Methods and Applications, 2017, 10(1):1-21.

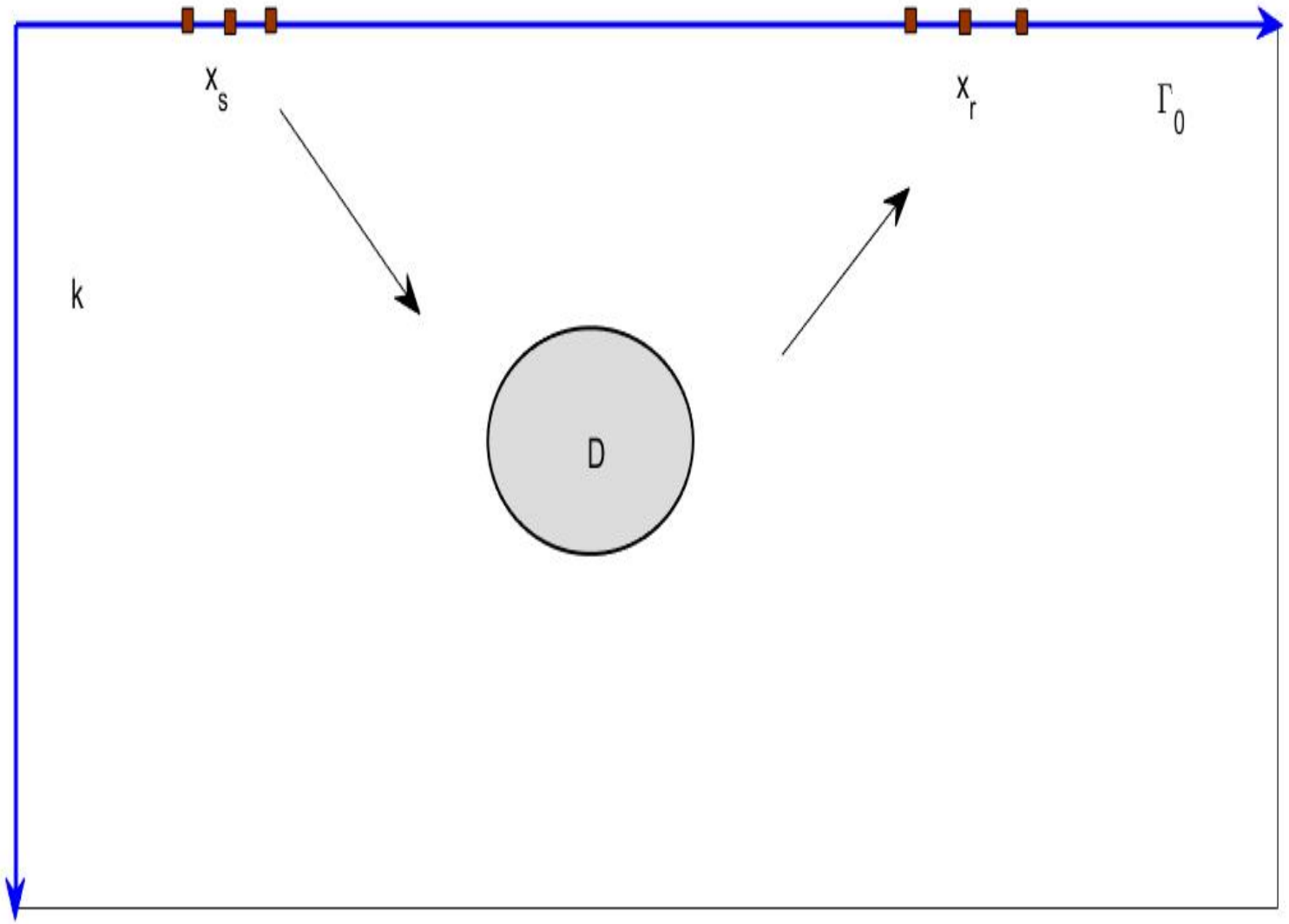
x_s
x_r
Γ_0
k
D

RTM Algorithm

Given the data $u_k^s(x_r, x_s)$, $k = 1, 2$ which is the measurement of the scattered field at x_r when the source is emitted at x_s along the polarized direction e_k, $s = 1, \ldots, N_s$ and $r = 1, \ldots, N_r$.

$$I_d(z) = \mathrm{Im} \sum_{k=1}^{2} \left\{ \frac{|\Gamma_0^d|}{N_s} \sum_{s=1}^{N_s} \sum_{i=1}^{2} [\sigma_{x_s}(\mathbb{D}(x_s, z)e_i)e_2 \cdot e_k][v_k(z, x_s) \cdot e_i] \right\}. \quad z \in \Omega \qquad (1)$$

where $v_k(z, x_s)$ satisfy the following scattering elastic equation:

$$\Delta_e v_k(z, x_s) + \omega^2 v_k(z, x_s) = 0 \qquad \text{in } \mathbb{R}^2_+$$

$$v_k(z, x_s) = \frac{|\Gamma_0^d|}{N_r} \sum_{r=1}^{N_r} \overline{u_k^s(x_r, x_s)} \delta_{x_r}(z) \qquad \text{on } \Gamma_0$$

By letting $N_s, N_r \to \infty$, we know that (1) can be viewed as an approximation of the following continuous integral:

$$\hat{I}_d(z) = \mathrm{Im} \sum_{q=e_1,e_2} \int_{\Gamma_0^d} \int_{\Gamma_0^d} [\mathbb{T}_D(x_s, z)^T q][\mathbb{T}_D(x_r, z)^T \overline{u_q^s(x_r, x_s)}] \, ds(x_r) ds(x_s).$$

where $z \in \Omega$.

Point Spread Function

The point spread function measures the resolution to find a point source. Given the $\mathbb{N}(x,y)$ on $\Gamma_0^d = \{(x_1,x_2)^T \in \Gamma_0,\ x_1 \in (-d,d)\}$ with the source $y \in \mathbb{R}^2_+$, we define the PSF as the back-propagated field $\mathbb{J}_d(x,y)$.

$$\Delta_e \mathbb{J}_d(x,y) + \omega^2 \mathbb{J}_d(x,y) = -\delta_y(x)\mathbb{I} \quad in \quad \mathbb{R}^2_+, \quad \mathbb{J}_d(x,y) = \mathbb{N}(x,y)\chi_{(-d,d)} \qquad on \quad \Gamma_0$$

By integral representation

$$\begin{aligned}
\mathbb{J}_d^{ij}(z,y): &= e_i \cdot \mathbb{J}_d(z,y)e_j \\
&= \int_{\Gamma_0^d} \sigma_x(\mathbb{D}(x,z)e_i)e_2 \cdot \overline{\mathbb{N}(x,y)}e_j ds(x) \\
&= \int_{-d}^{d} \sigma_x(\mathbb{D}(x_1,0;z_1,z_2)e_i)e_2 \cdot \overline{\mathbb{N}(x_1,0;y_1,y_2)}e_j dx_1
\end{aligned}$$

Numerical test: PSF

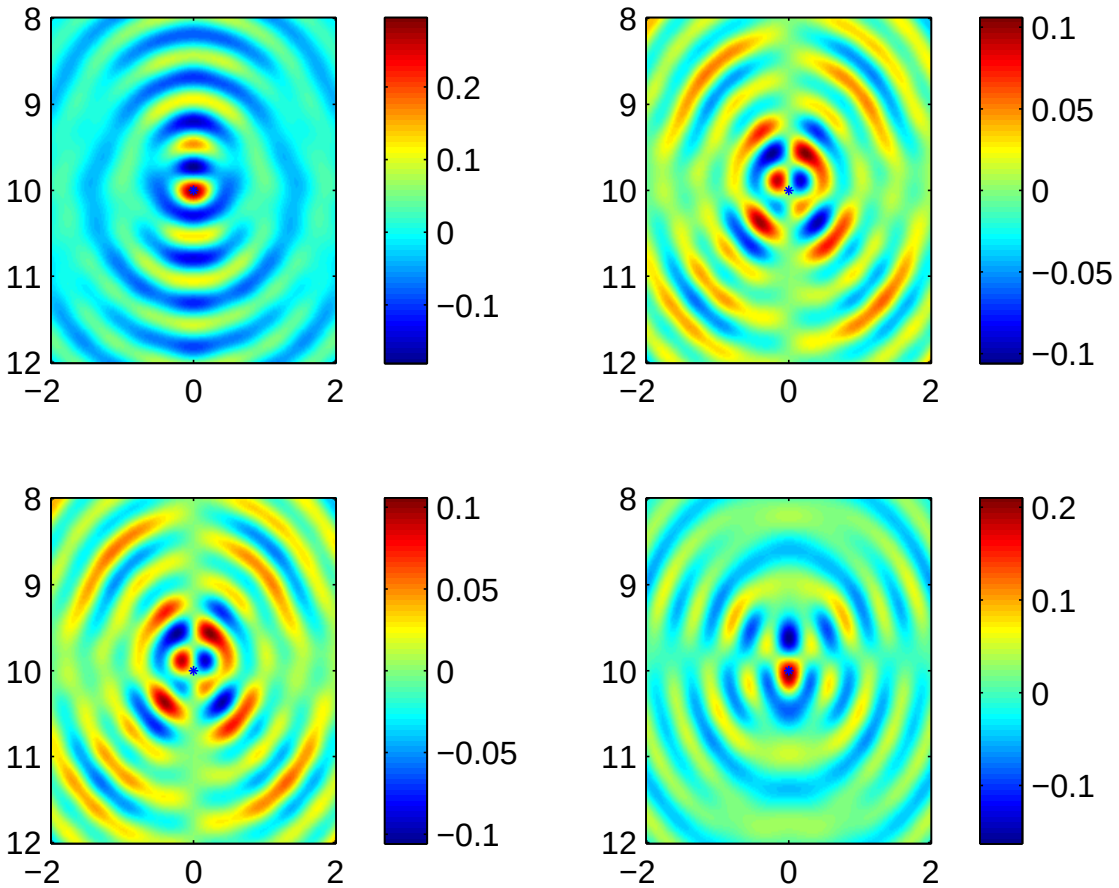

Figure: The figures on the diagonal line show that psf have peaks on the point x=y

Analysis of PSF

Hypothesis

We assume the obstacle $D \subset \Omega$ and there exist constants $0 < c_1 < 1, c_2 > 0, c_3 > 0$ such that

$$h < d, \quad |x_1| \leq c_1 d, \quad |x_1 - y_1| \leq c_2 h, \quad |x_2| \leq c_3 h \quad \forall x, y \in \Omega$$

Theorem 1

Let $k_s h > 1$. For any $z, y \in \Omega$, PSF can be reprsented by $J_d(z, y) = \mathbb{F}(z, y) + \mathbb{R}(z, y)$ and it satisfy that

$$|\mathbb{R}_{ij}(z,y)| + k_s^{-1}|\nabla_y \mathbb{R}_{ij}(z,y)| \leq \frac{C}{\mu}\left(\frac{1}{(k_s h)^{\frac{1}{2n^*}}} + k_s h e^{-k_s h\sqrt{\kappa_R^2 - 1}}\right) + \frac{C}{\mu}\left(\left(\frac{h}{d}\right)^2 + \frac{(k_s h)^{1/2}}{e^{k_s h\sqrt{\kappa_R^2-1}}}\left(\frac{h}{d}\right)^{1/2}\right)$$

uniformly for $z, y \in \Omega$. Here $\kappa_R := k_R/k_s$ and the constant C may dependent on $k_s d_D$ and $\kappa := k_p/k_s$, but is independent of k_s, k_p, h, d_D.

Main Term of PSF

Based on the above argument, we know that $\mathbb{R}(z,y)$ becomes small when z,y move away from Γ_0 and $d \gg h$. Our goal is to show $\mathbb{F}(z,y)$ has the similar decay to the elastic fundamental solution $\operatorname{Im}\Phi(z,y)$ as $|z-y| \to \infty$.

Theorem 2

For any $z, y \in \mathbb{R}^2_+$, when $z = y$

$$|\operatorname{Im}\mathbb{F}_{ii}(z,y)| \geq \frac{1}{4(\lambda+2\mu)} \ , \ i = 1,2$$
$$\operatorname{Im}\mathbb{F}_{12}(z,y) = \operatorname{Im}\mathbb{F}_{21}(z,y) = 0$$

and for $z \neq y$

$$|\mathbb{F}_{ij}(z,y)| \quad \leq \frac{C}{\mu}[(k_s|z-y|)^{-1/2}) + (k_s|z-y|^{-1})]$$

where constant C is only dependent on $\kappa := k_p/k_s$.

Now, We turn to study the resolution of the function $\hat{I}_d(z)$. To do this, we first show the difference between the half space scattering solution and the full space scattered solution is small if the scatterer is far away from the boundary Γ_0.

Theorem 3

Let $g \in H^{1/2}(\Gamma_D)$ and $\mathbf{u}_1, \mathbf{u}_2$ be the scattering solution of following problems:

$$\begin{aligned} \Delta_e \mathbf{u}_1 + \omega^2 \mathbf{u}_1 = 0 \quad & \text{in } \mathbb{R}^2_+ \backslash \bar{D} \\ \mathbf{u}_1 = g \quad & \text{on } \Gamma_D \\ \sigma(\mathbf{u}_1) e_2 = 0 \quad & \text{on } \Gamma_0 \end{aligned}$$

and

$$\begin{aligned} \Delta_e \mathbf{u}_2 + \omega^2 \mathbf{u}_2 = 0 \quad & \text{in } \mathbb{R}^2 \backslash \bar{D} \\ \mathbf{u}_2 = g \quad & \text{on } \Gamma_D \end{aligned}$$

Then there exits a constant C independent of k_s, k_p, such that

$$\|\sigma_x(\mathbf{u}_1 - \mathbf{u}_2)\nu\|_{H^{-1/2}(\Gamma_D)} \leq \frac{C}{\mu}(1 + \|T_f\|)(1 + \|T_h\|)(1 + k_s d_D)^2 \epsilon_1(k_s h)\|g\|_{H^{1/2}(\Gamma_D)}$$

Resolution Analysis

Theorem 4

For any $z \in \Omega$, let $\Psi(y,z) \in \mathbb{C}^{2\times 2}$ be the radiation solution of the problem:

$$\Delta_e \Psi(y,z)e_i + \omega^2 \Psi e_i = 0 \quad \text{in } \mathbb{R}^2_+ \backslash \bar{D} \quad i = 1,2$$
$$\Psi(y,z) = -\overline{\mathbb{F}(z,y)} \qquad \text{on } \Gamma_D$$

Then, we have

$$\hat{I}_d(z) = \mathrm{Im} \int_{\Gamma_D} \sum_{i=1}^{2} [\sigma_y((\overline{\mathbb{F}(z,y)} + \Psi(y,z))e_i) \cdot \overline{\mathbb{F}(z,y)e_i}] ds(y) + \mathbb{W}_{\hat{I}}(z) \tag{2}$$

where $|\mathbb{W}_{\hat{I}}(z)| \leq \frac{C}{\mu}(1+\|T_f\|)(1+\|T_h\|)(1+k_s d_D)^4(\epsilon_1(k_s h) + \epsilon_2(k_s h, h/d))$ uniformly for z in Ω.

Numerical Test: Different Boundary Condition

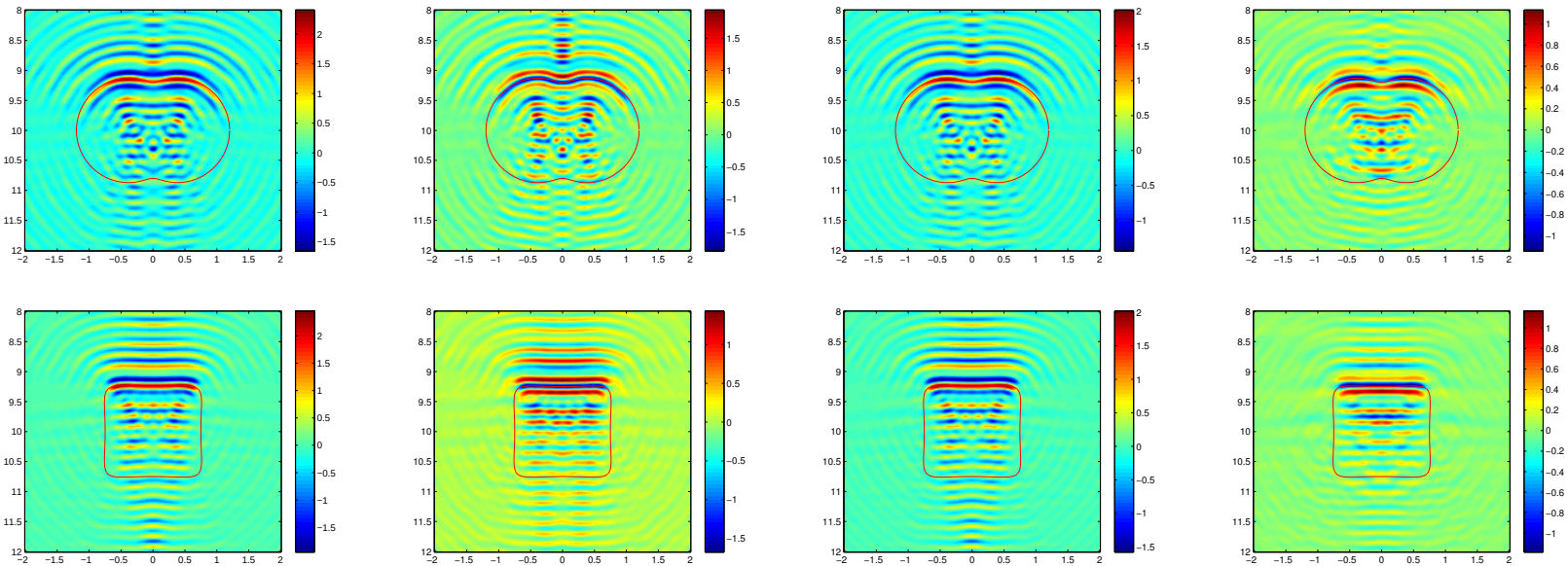

Figure: Example 1: From left to right: imaging results of a Dirichlet, a Neumann, a Robin bounday with impedance $\eta(x) = 1$, and a penetrable obstacle with diffractive index $n(x) = 0.25$

Numerical Test: Different Sharp

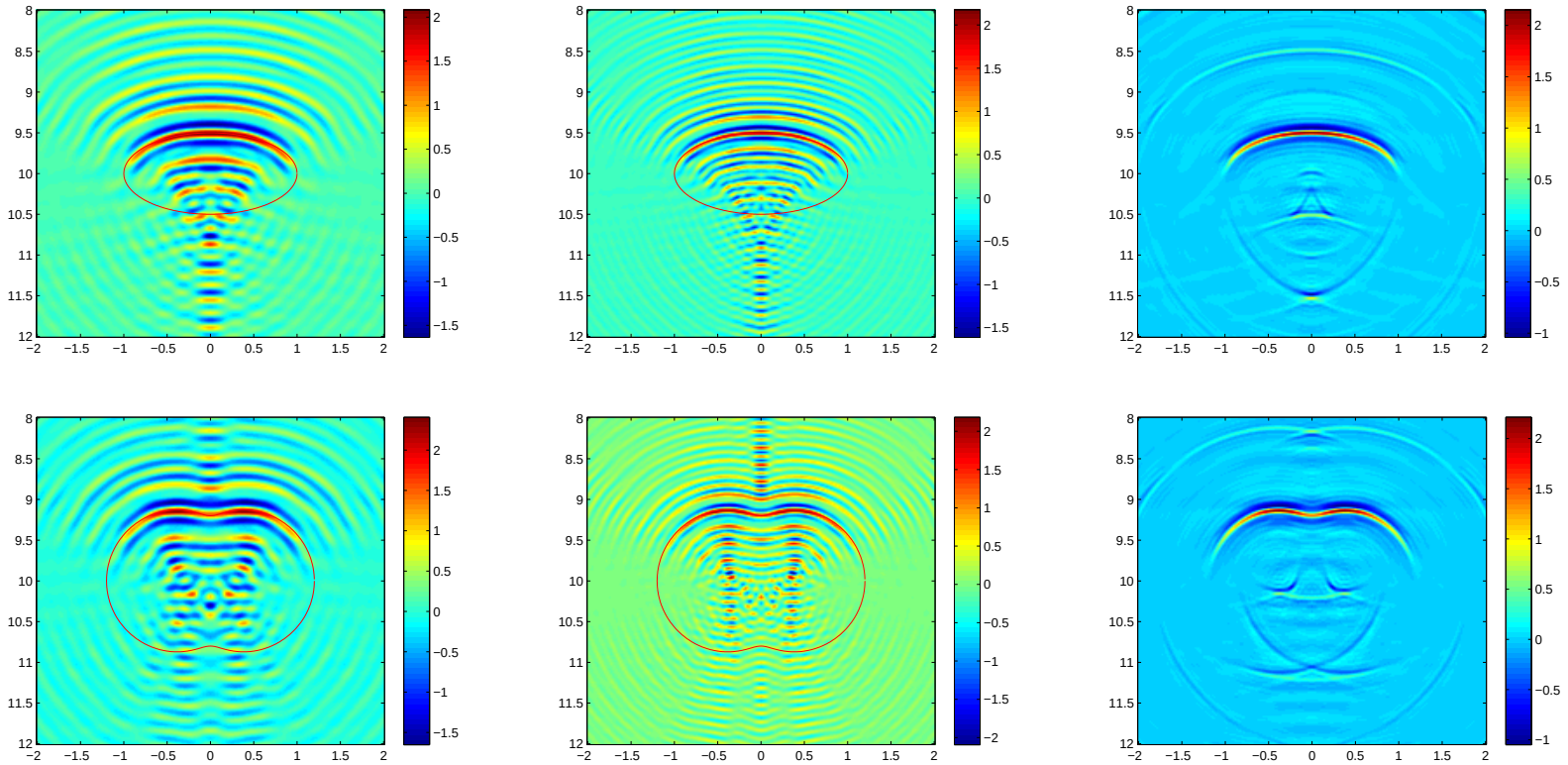

Figure: Example 2: Imaging results of clamped obstacles with different shapes from top to below. The left row is imaged with single frequency data where $\omega = 3\pi$, The middle row is imaged with single frequency data where $\omega = 5\pi$ and The left row is imaged with multi frequency data

Numerical Test: Different Sharp

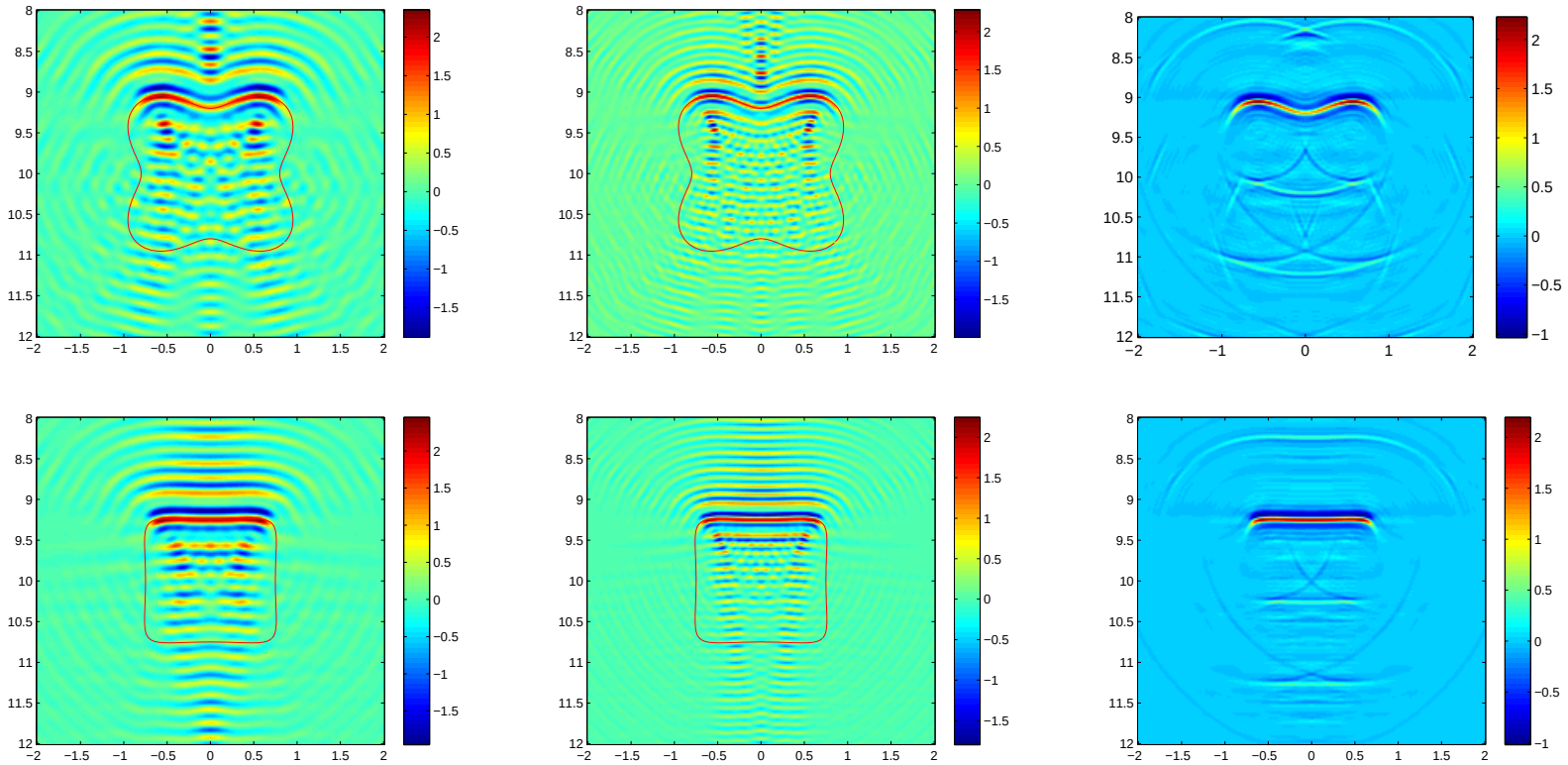

Figure: Example 3: Imaging results of clamped obstacles with different shapes from top to below. The left row is imaged with single frequency data where $\omega = 3\pi$, The middle row is imaged with single frequency data where $\omega = 5\pi$ and The left row is imaged with multi frequency data

Numerical Test: Two Obstacles

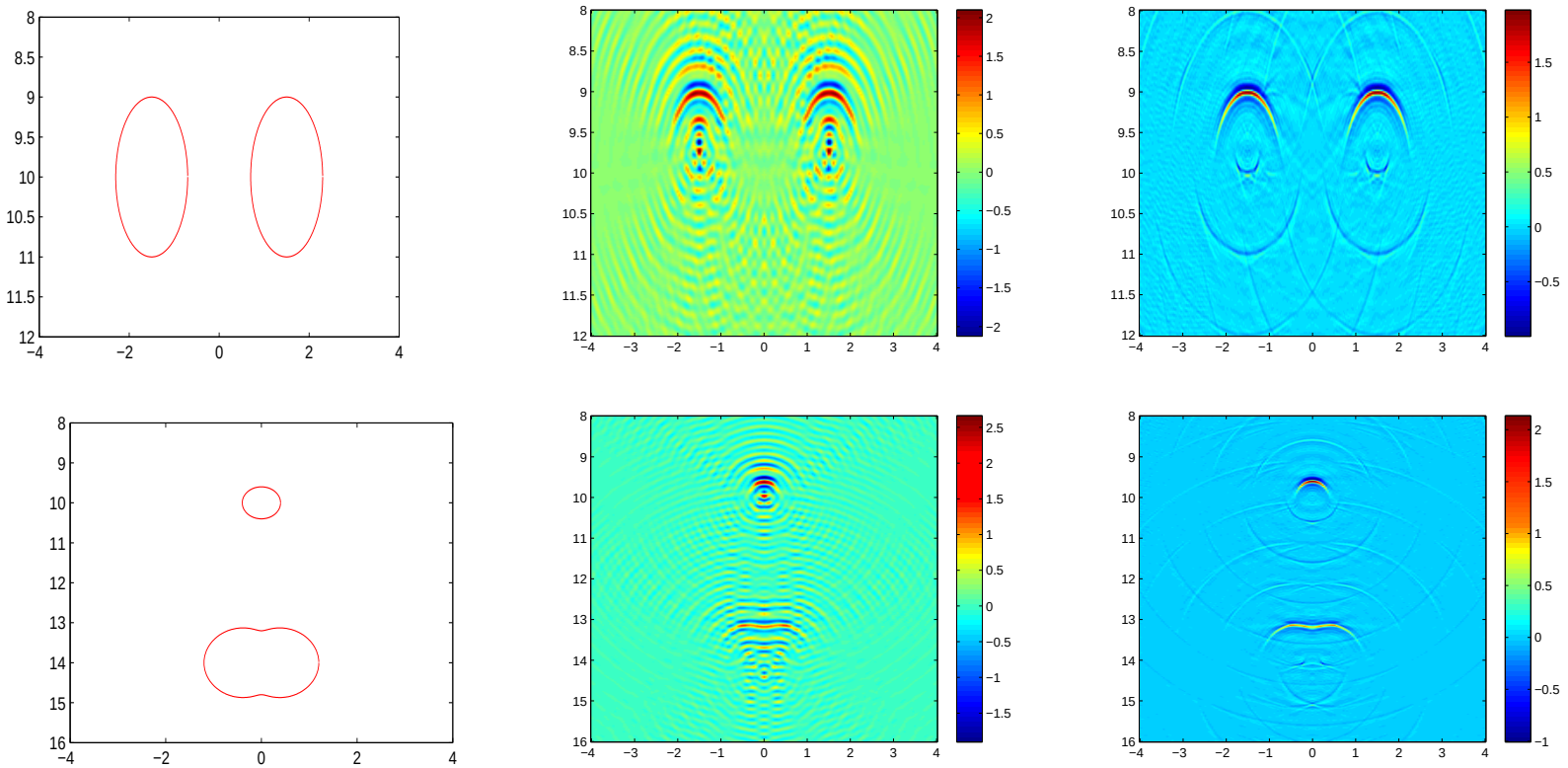

Figure: Example 4:From left to right, true obstacle model with two circles. the imaging result with single frequency data where $\omega = 3\pi$, the imaging result with multiple frequency data.

Numerical Test: additive Gaussian noise

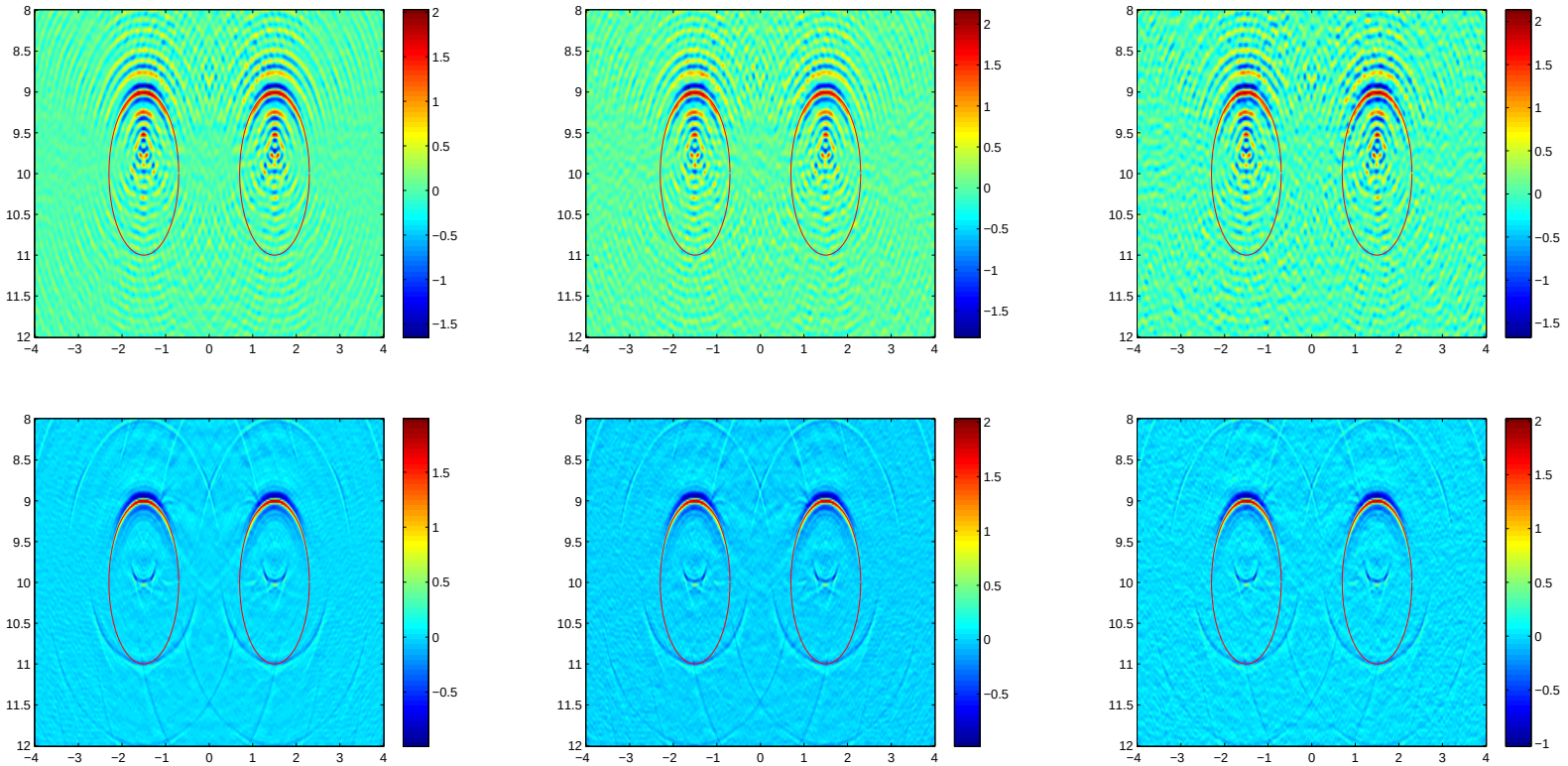

Figure: Example 5: Imaging results of a clamped obstacle with noise levels $\mu = 0.2; 0.3; 0.4$ (from left to right). The top row is imaged with single frequency data where $\omega = 4\pi$, and the bottom row is imaged with multi-frequency data.

Physical interpretation: high frequence

Let y(s) be the arc length parametrization of the boundry Γ_D and $y_\pm(\eta_\theta) = y(s_\pm)$ be the pionts such that $\nu(y(s_\pm)) = \pm\eta_\theta$ and $\eta(y)$ be Gauss curvature. In the case of $\omega \gg 1$, by stationary phase theorem and Kirchhoff approximation, the imaging function for the clamped obstacle is

$$\begin{aligned}\hat{I}_d(z) \quad &\approx \quad \sqrt{8\pi k_p}\mathrm{Im}\,\mathbf{tr}\int_0^\pi ((\lambda+2\mu)A_p(\theta)\eta_\theta e^{\mathbf{i}k_p(y_-(\eta_\theta)-z)\cdot\eta_\theta - \mathbf{i}\frac{\pi}{4}})^T \frac{\overline{F(z,y_-(\eta_\theta))}}{\sqrt{\vartheta(y_-(\eta_\theta))}}d\theta \\ &+ \quad \sqrt{8\pi k_s}\mathrm{Im}\,\mathbf{tr}\int_0^\pi (\mu A_s(\theta)\eta_\theta^\perp e^{\mathbf{i}k_s(y_-(\eta_\theta)-z)\cdot\eta_\theta - \mathbf{i}\frac{\pi}{4}})^T \frac{\overline{F(z,y_-(\eta_\theta))}}{\sqrt{\vartheta(y_-(\eta_\theta))}}d\theta\end{aligned}$$

Now for z in the part of Γ_D which is back to Γ_0, ie $\nu(z)\cdot\eta_\theta > 0$ for any $\theta \in [0,\pi]$, we know that z and $y_-(\eta_\theta)$ are far away and thus $\hat{I}_d(z) \approx 0$. By above formula , we can explain that one cannot image the back part of the obstacle with only the data collected on Γ_0. This confirmed in our numerical examples.

Our work:

- New form and asymptotic analysis of Green tensor in the half space..
- Regularity estimate of direction elastic wave equation in the Half-space.
- Mathematics analysis of point spread function.
- Resolution analysis of Reverse Time Migration without any geometric optics approximation .
- Scattered wave data simulation and numerical test of RTM.

Publication:

- Chen Z, Zhou S. *Reverse time migration for reconstructing extended obstacles in the half space: Elastic Waves.* submitted.
- Chen Z, Zhou S. *A Direct Imaging Method for Half-space Inverse Elastic Scattering Problems.* submitted.
- Chen Z, Zhou S. *A Direct Imaging Method for Half-space Inverse Elastic Scattering Problems with Phaseless Data.* Preprint.
- Chen Z, Zhou S. *Absense of Positive Eigenvalues for the Linearized Elasticity System in the Half Space* Preprint

Thank you !